4-2

LOW NOISE HIGH ELECTRON MOBILITY TRANSISTORS

J. J. Berenz, K. Nakano, and K. P. Weller

TRW Electronic Systems Group
One Space Park
Redondo Beach, CA 90278

ABSTRACT

Sub-half-micron gate length High Electron Mobility Transistors (HEMT) were fabricated by direct-write electron beam lithography for low noise EHF amplifiers. Modulation-doped epitaxial structures were grown by molecular beam epitaxy having 8,000 cm^2/V-sec room temperature and 77,600 cm^2/V-sec liquid nitrogen Hall mobility for 10^{12} electrons/cm^2. Gate lengths as narrow as 0.28 micron were defined in a recess etched through the n^+ GaAs contact layer. The dc transconductance of 0.4 micron gate length depletion mode devices exceeded 260 mS/mm. Preliminary measurement of noise figure and associated gain made at room temperature yielded 2.7 dB noise figure and 5.9 dB associated gain at 34 GHz for devices having 0.37 micron gate length. Enhancement mode devices were also fabricated having 240 mS/mm dc transconductance. These devices yielded 1.5 dB noise figure and 10.5 dB associated gain at 18 GHz for 0.35 micron gate length. These results are comparable to the best quarter-micron gate length GaAs MESFET noise figures yet reported.[1,2]

Introduction

Increasing demands on the performance required of millimeter wave receivers has led us to the development of discrete ultra low noise, low power dissipation High Electron Mobility Transistors for use in hybrid MIC pre-amplifiers. These pre-amplifiers can be used ahead of existing diode mixer and associated local oscillator circuitry to establish the noise figure of the receivers. High Electron Mobility Transistors have been fabricated which demonstrate the potential for noise performance superior to GaAs MESFETs. In this paper we describe the design, fabrication, evaluation, and performance of these HEMT devices.

Design

The principal factors governing device noise figure are described by the Fukui noise figure equation in Figure 1. The equivalent circuit elements used in the equation are related to the physical regions of the HEMT device structure as shown in Figure 2. The gate-source capacitance, C_{GS}, is the principal factor governing noise figure; it is dominated by the channel capacitance, C_c. This capacitance can be minimized by reducing the gate length and optimizing the vertical channel doping profile. The intrinsic transconductance G_m is also primarily determined by the details of the epitaxial structure. Thus, the gate length and epitaxial structure primarily determine the noise figure. Minimizing the ratio of $C_{GS}/\sqrt{G_m}$ minimizes the noise figure. The source resistance, R_s, and gate metal resistance, R_G, are parasitic elements which also contribute to the noise figure. Their contribution can be significant, particularly at high frequency. On the other hand, the transistor gain is primarily determined by the cutoff frequency, f_T, which is given by the following expression:

$$f_T = \frac{G_m}{2\pi C_{GS}} \quad . \qquad (1)$$

To first order, the power gain depends on the cutoff frequency according to the following expression:

$$G = \left(\frac{f_T}{f}\right)^2 \quad , \qquad (2)$$

where f is the operating frequency. Thus, to maximize the power gain, it is necessary to minimize the ratio C_{GS}/G_m. Although the functional dependence of gain on transconductance is greater than for the noise figure, both noise figure and gain are affected in the same manner by the ratio of these quantities.

Gate length, gate width, and electrode topology selections were made in conjunction with the design of the epitaxial structure and the selection of the fabrication technology needed to achieve low parasitic elements and high cutoff frequency. These key factors determine the noise figure and gain of the transistor.

Fabrication

Sub-half-micron gate length High Electron Mobility Transistors were fabricated by direct-write electron beam lithography on modulation-doped epitaxial structures grown by molecular beam epitaxy. The epitaxial structures were grown in a Varian MBE/Gen II system on 2-inch diameter undoped LEC substrates. To achieve high device transconductance, while maintaining high electron mobility, a thin 20 Å undoped $Al_{0.3}Ga_{0.7}As$ "spacer layer" was grown to separate the two-dimensional electrons from their ionized "parent" donors, as

0149-645X/84/0000-0187 $01.00 © 1984 IEEE

shown in Figure 3. Typical room temperature Hall mobilities were 7700 cm^2/V-sec for 10^{12} electrons/cm^2, while liquid nitrogen temperature Hall mobilities were typically 69,000 cm^2/V-sec. The best values measured are given in the abstract.

Discrete low noise transistors were fabricated with $\leq$ 0.4 micron gate length and nominal 75 micron total gate width. Three different transistor topologies were evaluated having multiple gate feeds and short gate finger widths to minimize losses at high frequency. Device active areas were isolated by etching mesas to a depth of 2500 Å. Source and drain ohmic contact areas were defined by photolithography. Ni/AuGe/Ni/Au contact metals were evaporated, "lifted-off," and alloyed to form source and drain ohmic contacts. Note that nickel was deposited first to assist in driving the Ge through the AlGaAs layer to make a low resistance contact to the buried two-dimensional electron gas layer.

The definition of gates for HEMT devices was performed by e-beam lithography using TRW's Cambridge EBMF-2 e-beam exposure system. We have demonstrated satisfactory PMMA resist images for lift-off of thin $<$ 0.25 μm long aluminum gates. Best results were obtained with low electron beam currents (1 nA) and with a single pass of the electron beam (i.e., a single line of exposure points), as demonstrated by the SEM photograph of a 0.4-micron long gate shown in Figure 4. The dark area surrounding the light colored gate stripe is the channel recess etched through the n^+ GaAs contact layer. The recessed gate is situated closer to the source contact in a 1.8-micron channel between source and drain contacts. Either depletion-mode or enhancement-mode transistor operation was achieved, depending on the depth of the gate recess. The recess depth was gauged by monitoring the drain-source saturation current during etching.

Evaluation

The dc and rf characteristics of the High Electron Mobility Transistors have been measured and analyzed to determine device parameters. DC I-V characteristics were analyzed using the University of Illinois analytical device model.(3) A typical fit to the measured DC I-V characteristics of an enhancement mode transistor is shown in Figure 5. The dc transconductance is 240 mS/mm. The rise in drain current with drain voltage in the saturation regime (i.e., low output resistance) is due to dynamic effects not included in the model.

Small-signal S-parameters of the transistors were measured in a 50-ohm microstrip test fixture over the 2-18 GHz frequency range. An equivalent circuit was determined using COMPACT* optimization to fit the elements of the equivalent circuit shown in Figure 6 to the measured S-parameter data. Table 1 lists a typical result. The inferred source resistance is relatively low (0.38 ohm-mm), but the gate resistance is high (37 ohms/mm) due to the thin gate metal used (2500 Å). The input resistance is also much higher than a comparable depletion-mode GaAs MESFET. In spite of these limitations, an excellent device noise figure of 1.5 dB was measured at 18 GHz for this HEMT device. And, it should be noted that relatively high associated gain (10.5 dB) was achieved at a much lower drain-source current level (3.7 mA) than GaAs MESFETs exhibiting comparable low noise performance. This is an extremely important advantage of HEMT devices over GaAs MESFETs.

Performance

Table 2 summarizes the best noise figure performance measured for the nominal 0.35-micron gate length High Electron Mobility Transistors. In spite of their longer gate length, higher gate metal resistance, and higher channel resistance, these HEMT devices exhibit noise figures comparable to the best reported for quarter micron gate length GaAs MESFETs. This being the case, ultimately lower noise figures than GaAs MESFETs should be achievable with HEMT devices having narrower gate lengths and improved parasitic elements.

In order to estimate the magnitude of the improvement possible, we extended the analytical device model to compute noise figure and gain from the device physical parameters. Excellent agreement has been obtained between calculated and measured noise performance in the case of the experimental devices which we analyzed. Theoretically, depletion-mode HEMT devices should exhibit lower noise figures than their enhancement-mode counterparts because of higher transconductance and lower gate-source capacitance. Figure 7 compares the calculated noise figure for the experimental depletion-mode devices with the measured noise figures. The noise performance projected for an optimized 0.25-micron gate length depletion-mode device at room temperature is also plotted in this figure to show the magnitude of the improvement theoretically possible. This projection of HEMT device noise figure is lower than the best measured noise figures for GaAs MESFETs and the magnitude of the improvement in noise figure over GaAs is greater at higher frequencies.

Conclusions

High Electron Mobility Transistors have been fabricated which demonstrate the potential for lower power dissipation, lower noise amplification than GaAs. As a result, these devices are expected to play a major role in future microwave and millimeter-wave monolithic receiver circuits.

References

1. P. W. Chye and C. Huang, "Quarter Micron Low Noise GaAs FET's," IEEE Electron Device Letters, Vol. EDL-3, No. 12, December 1982, pp. 401-403.

*Trademark of Compact Engineering, Palo Alto, CA.

2. M. Feng, H. Kanber, V. K. Eu, E. Watkins, and L. R. Hackett, "Ultrahigh Frequency Operation of Ion Implanted GaAs Metal-Semiconductor Field-Effect Transistors," Appl. Phys. Lett., Vol. 44, No. 2, 15 January 1984, pp. 231-233.

3. T. J. Drummond, H. Morkoc, K. Lee, and M. Shur, "Model for Modulation Doped Field Effect Transistor," IEEE Electron Device Letters, Vol. EDL-3, No. 11, November 1982, pp. 338-341.

$$NF = 1 + 2\pi C_{GS} KF \sqrt{\frac{R_S + R_G}{G_M}}$$

WHERE

- G_M = TRANSCONDUCTANCE (mS/mm) $\leq 1/R_C$
- C_{GS} = GATE-SOURCE CAPACITANCE (pF/mm) $\sim C_c$
- R_s = SOURCE RESISTANCE (OHM mm)
- R_G = GATE SERIES RESISTANCE (OHM/mm)
- K = FACTOR RELATED TO MATERIAL TYPE
  - K = 2.5 GaAs
  - K = 1.6 HEMT
- F = FREQUENCY (GHz)

Figure 1. Fukui Noise Figure Equation

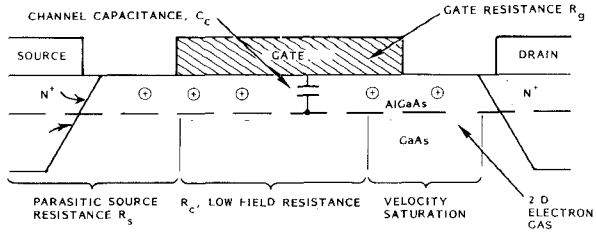

Figure 2. HEMT Cross-Section

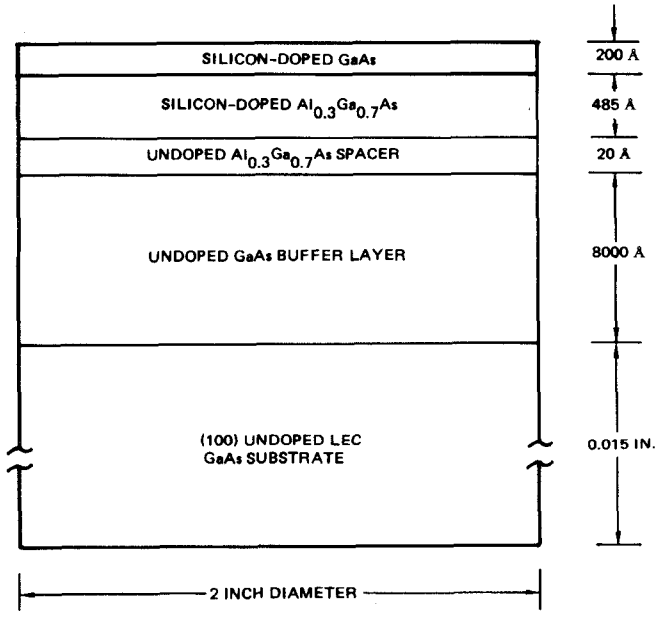

Figure 3. MBE-Grown Modulation-Doped Epitaxial Structure

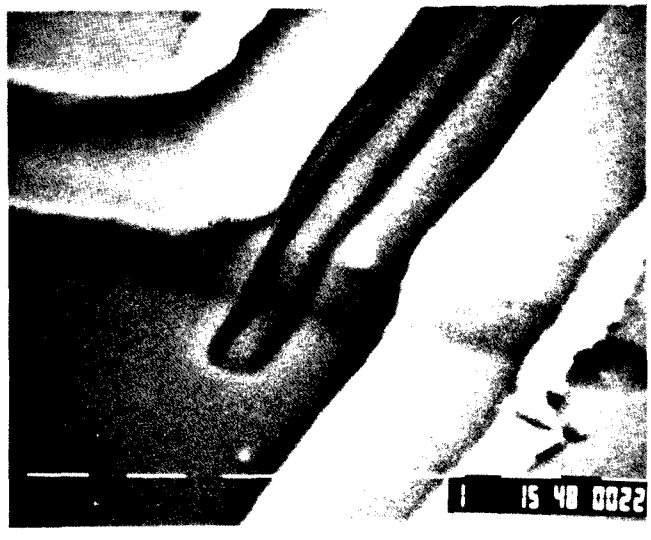

Figure 4. SEM Photo of HEMT Channel

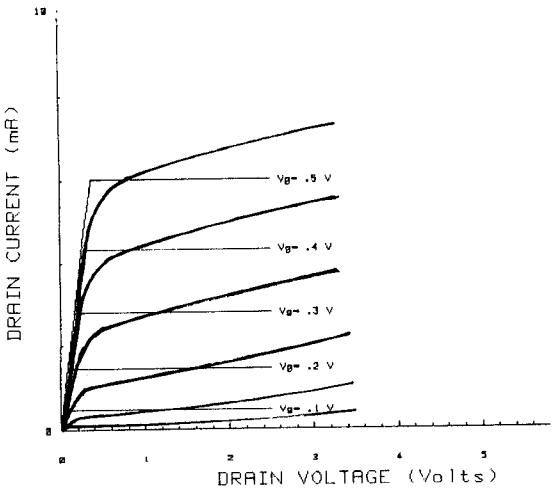

Figure 5. Comparison of Measured and Calculated I-V Characteristics of Enhancement Mode HEMT

Table 2.

TRW HEMT DEVICE PERFORMANCE

RESULT					
NF (dB)	G_{ASS} (dB)	F (GHz)	MBE LAYER NO.	DEVICE TYPE	GATE LENGTH
1.3	9.0	15	2067	DEPLETION MODE	0.35 μm
1.5	10.5	18	2078	ENHANCEMENT MODE	0.35
2.7	5.9	34	2067	DEPLETION MODE	0.35

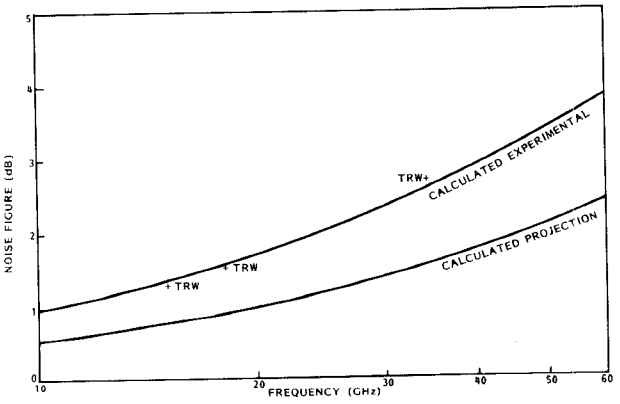

Figure 7. HEMT Noise Figure Versus Frequency

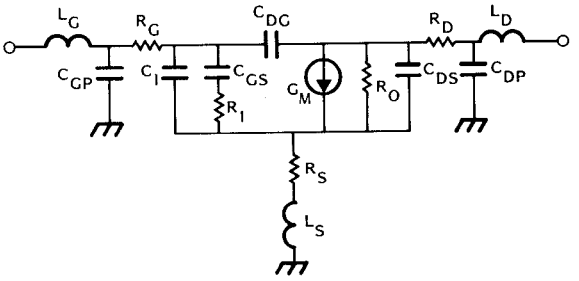

Figure 6. Equivalent Circuit

Table 1. Equivalent Circuit Element Values

Parameter	HEMT 2078
TYPE	E-mode
Geometry	Pi-gate
Gate Length	0.35
Gate width	65
NF (dB)	1.5
Gass (dB)	10.5
Freq (GHz)	18
Id (mA)	3.7
Vd (V)	3.0
Vg (V)	0.5
ELEMENTS	
Lg (nH)	.18
Cgp (pF)	.012
Rg (ohms)	2.4
Cin (pF)	.011
Cgs (pF)	.051
Rin (ohms)	17.1
Rs (ohms)	5.9
Ls (nH)	.076
Cds (pF)	.0108
Ro (ohms)	673
Gm (mS)	15
Cdg (pF)	.0148
Rd (ohms)	6.0
Cdp (pF)	.0088
Ld (nH)	.26